Rotationally resolved threshold photoelectron spectra of OH and OD

R. T. Wiedmann, R. G. Tonkyn, M. G. White, Kwanghsi Wang, and V. McKoy

Citation: The Journal of Chemical Physics **97**, 768 (1992); doi: 10.1063/1.463179
View online: http://dx.doi.org/10.1063/1.463179
View Table of Contents: http://scitation.aip.org/content/aip/journal/jcp/97/2?ver=pdfcov
Published by the AIP Publishing

Rotationally resolved threshold photoelectron spectra of OH and OD

R. T. Wiedmann, R. G. Tonkyn,[a] and M. G. White
Chemistry Department, Brookhaven National Laboratory, Upton, New York 11973

Kwanghsi Wang and V. McKoy
Arthur Amos Noyes Laboratory of Chemical Physics,[b] California Institute of Technology, Pasadena, California 91125

(Received 28 February 1992; accepted 10 April 1992)

The results of combined experimental and theoretical studies of the rotationally resolved photoelectron spectra of OH and OD following single-photon ionization are presented. The measured zero-kinetic-energy (ZEKE) spectra were obtained using pulsed field ionization in conjunction with a vacuum ultraviolet laser source. The OH^+ and OD^+ ($X\,^3\Sigma^-$, $v^+=0$) rotational distributions were studied over the range 95.0–95.4 nm. Agreement between the observed and calculated spectra is very encouraging. Improved values for the ionization potentials of OH and OD (104 989 and 105 085 ± 2 cm^{-1}, respectively) are reported and the unusual dynamics favoring $\Delta N<0$ transitions are discussed.

I. INTRODUCTION

In a continuing study of rotationally resolved photoionization of small molecules, we focus our attention on the fundamentally important radical OH and its isotope OD. The large rotational constants of the neutral and cation species make OH well suited for rotationally resolved VUV photoionization studies, particularly since most radical sources result in thermal or super-thermal ground state rotational distributions. Previous single-photon photoelectron measurements on OH have been hampered by the difficulty of isolating the OH spectrum from that of excess reactants and products present in microwave discharge, flow-tube radical sources.[1,2] Through a combination of spectrum stripping and modulation technique, Lonkhuyzen and de Lange[2] obtained the complete He I ($h\nu=21.2$ eV) photoelectron spectra for OH (OD) at moderate resolution (~45 meV) from which approximate ionization potentials and cation vibrational frequencies were derived. Much more recently, de Beer *et al.*[3,4] have used laser photolysis of H_2O_2 and resonant multiphoton ionization to record high-resolution photoelectron spectra for ionization of the $D\,^2\Sigma^-$ and $3\,^2\Sigma^-$ excited electronic states. These spectra exhibited partially resolved rotational structure which was interpreted on the basis of *ab initio* calculations. These calculations suggest that Cooper minima in specific photoelectron matrix elements are responsible for the unusual rotational state distribution observed for ionization via the $D\,^2\Sigma^-$ state.

In this paper we present rotationally resolved threshold photoelectron spectra of OH and OD, obtained using pulsed field ionization (PFI) in conjunction with a high resolution coherent VUV radiation source. With this technique, successive ionization thresholds are detected by field ionizing molecules excited to Rydberg levels with very high principal quantum number (n) lying within 1–2 cm^{-1} of their respective ionization limits.[5,6] The overall resolution is determined largely by the VUV laser radiation bandwidth (~1 cm^{-1}) which represents a considerable improvement over previous photoelectron measurements. By selectively detecting only high-n Rydberg states which generally correspond to only one molecular species, PFI can in many cases detect dilute species (e.g., radicals) in a bath of interfering gases. Such conditions exist for detecting OH (OD) in the flow-tube source used here and "clean" ionization spectra of these radicals are obtained without spectrum stripping. These rotationally resolved spectra are compared with *ab initio* calculations using multiplet-specific final-state wave functions and an intermediate coupling scheme between Hund's cases (a) and (b) to represent the ground and ionic states.[7] Excellent agreement between calculated and measured spectra is seen. The mechanism favoring larger negative angular momentum changes ($\Delta N<0$) is also discussed.

II. EXPERIMENT

Figure 1 shows a schematic diagram of the time-of-flight spectrometer and discharge flow-tube radical source used in this work. The radicals OH and OD were formed through the rapid reaction of nitrogen dioxide and H atoms,[8] i.e., $NO_2+H\rightarrow OH+NO$. Hydrogen atoms were made in a flowing microwave discharge using a 15% H_2/85% He mixture. The flow tube consists of three concentric tubes located in the beam source chamber of the differentially pumped photoelectron spectrometer. Reactant NO_2 and the H/H_2/He mixture were introduced through the innermost and middle tubes, respectively. In order to prevent secondary reactions from depleting the OH product, the NO_2 and H atoms were combined very near the exit aperture of the flow tube. The outermost tube was connected to a mechanical pump, which controlled the overall flow rate and reduced the number of secondary reactions by minimizing the background pressure seen by the OH radicals. All surfaces that could come in contact with radical species (H, OH, and OD) were coated with

[a]Present Address: Materials and Chemical Sciences Center, Pacific Northwest Laboratory, Richland, Washington.
[b]Contribution No. 8581.

 0021-9606/92/140768-05$006.00

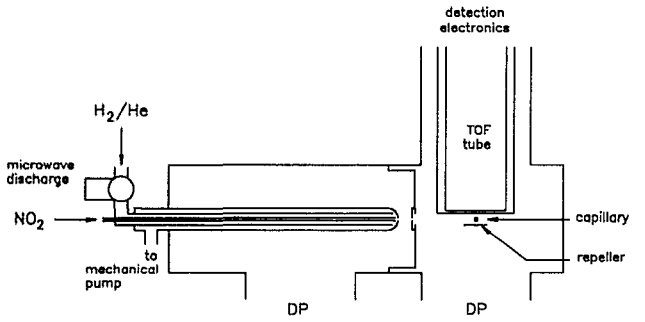

FIG. 1. The H atoms are made in the microwave discharge and react with NO_2 to form OH near the 1 mm opening at the end of the outermost tube. The OH radicals drift through a 3 mm hole into the ionization chamber where they are ionized by the VUV light exiting the capillary. Each chamber is pumped by a 6 in. diffusion pump.

phosphoric acid to reduce losses from wall collisions. The input pressures were typically 7–9 Torr for the H_2/He mixture and 1–2 Torr for NO_2. These pressures were chosen to maximize the OH^+ signal and minimize NO_2^+ and H_2O^+ (a secondary reaction product[9]), as determined from mass spectra taken with the spectrometer configured for detecting ions. Reaction products were expanded through a 1 mm hole and entered the spectrometer chamber through a 3 mm collimating aperture. The ambient pressure in the beam source chamber was $3–5\times10^{-4}$ Torr and $\sim3\times10^{-6}$ Torr in the spectrometer chamber.

The PFI technique consists of exciting molecules to the available Rydberg states near successive vertical ionization thresholds.[5,6] For 700–1000 ns after the laser pulse the excited molecules and prompt photoelectrons experience only a weak 50 mV/cm dc field, which serves to sweep any photoelectrons out of the ionization volume. A subsequent 0.5–0.6 V/cm pulsed field supplied by a digital delay/pulse generator (Stanford Research Systems Model DG 535) field ionizes the long-lived Rydberg states and accelerates the electrons into the flight tube where they are detected with a microchannel plate array detector.

Frequency tripling in a pulsed free-jet expansion of N_2 was used to produce coherent vacuum ultraviolet radiation between 95.0 and 95.4 nm.[10,11] A detailed description and evaluation of the apparatus has been published elsewhere.[12] The red dyes Rhodamine 590 and 610 were used alone and in mixtures to produce the tunable UV radiation (285.0–286.2 nm) necessary for third harmonic generation. UV pulse energies ranged from 2.5 to 10 mJ per pulse. The wavelength calibration of the dye laser was checked by measuring the two-photon (VUV+UV) resonance enhanced ionization signal from the well-known VUV absorptions in H_2.[13] The PFI spectra are corrected for the small Stark shift induced by the external pulsed field (~2 cm^{-1} for a 0.5 V/cm pulsed field) and all line positions have an estimated uncertainty of ±2 cm^{-1}.

III. THEORY AND NUMERICAL DETAILS

Under collision-free conditions, each M_J sublevel of a J rotational level is an independent channel for photoionization by linearly polarized light. Therefore, the differential cross section for photoionization of a rotational level can be written as

$$\frac{d\sigma}{d\Omega}\propto\sum_{M_JM_{J^+}}\rho_{M_JM_J}|\Gamma_{M_JM_{J^+}}|^2=\frac{\sigma}{4\pi}[1+\beta P_2(\cos\theta)], \tag{1}$$

where σ is the total cross section, β the asymmetry parameter, $P_2(\cos\theta)$ the Legendre polynomial, $|\Gamma_{M_JM_{J^+}}|^2$ the ionization probability out of the M_J magnetic sublevel leading to the M_{J^+} sublevel of the ion, and $\rho_{M_JM_J}$ the population in the M_J sublevel. The $X^2\Pi$ ground state of OH (OD) with its spin–orbit splitting constant $A=-139.21$ (-139.23) cm^{-1} and rotational constant $B=18.91$ (10.02) cm^{-1} is best described by the intermediate coupling scheme between Hund's cases (a) and (b).[14] An expression for $\Gamma_{M_JM_{J^+}}$ with an intermediate coupling scheme between Hund's cases (a) and (b) has been recently given by Wang and McKoy.[7]

There are three dipole-allowed transition channels $k\sigma$, $k\pi$, and $k\delta$ for photoionization of the 1π orbital of OH (OD) leading to the $X^3\Sigma^-$ ionic state. The multiplet-specific final-state continuum wave functions and corresponding static-exchange potentials have been given previously by Stephens and McKoy[15] in their studies of the rotationally and vibrationally unresolved cross sections and asymmetry parameters for photoionization of the valence orbitals of OH. The ground state wave function used here is obtained at the Hartree–Fock level at the equilibrium internuclear distance $R_e=1.834$ a_0. We used the Cartesian Gaussian basis of Ref. 15 augmented with five s and five p functions ($\alpha=0.06$, 0.03, 0.01, 0.005, and 0.002), and two d functions ($\alpha=0.036$ and 0.008) at the center of mass. The self-consistent-field energy in this basis was $-75.411\,177$ a.u. which agrees well with that of previous calculations.[15] For the final state, we use the frozen-core Hartree–Fock approximation, in which the ion–core orbitals are assumed to be identical to those of the ground state of OH (OD), and the photoelectron orbitals are obtained as solutions of Lippmann–Schwinger equations containing multiplet-specific static-exchange potential of the ion. The photoelectron (continuum) orbitals were obtained numerically using the iterative Schwinger variational method. Other details of the calculation can be found in Ref. 15.

IV. RESULTS AND DISCUSSION

A. Photoelectron spectra of OH

Figure 2 shows the measured and calculated rotationally resolved spectra for the photoionization of OH ($X^2\Pi_i$, $v''=0)\rightarrow OH^+$ ($X^3\Sigma^-$, $v^+=0)+e^-$. The agreement between the calculated and measured spectra is quite encouraging. A photoelectron kinetic energy of 25 meV is assumed in the calculations. Furthermore, we also assumed that the ground state is unaligned (i.e., all $M_{J''}$ sublevels are equally populated) and the e/f components of rotational levels of the ground state are equally populated. Note that alignment in the $M_{J''}$ sublevels and preference in

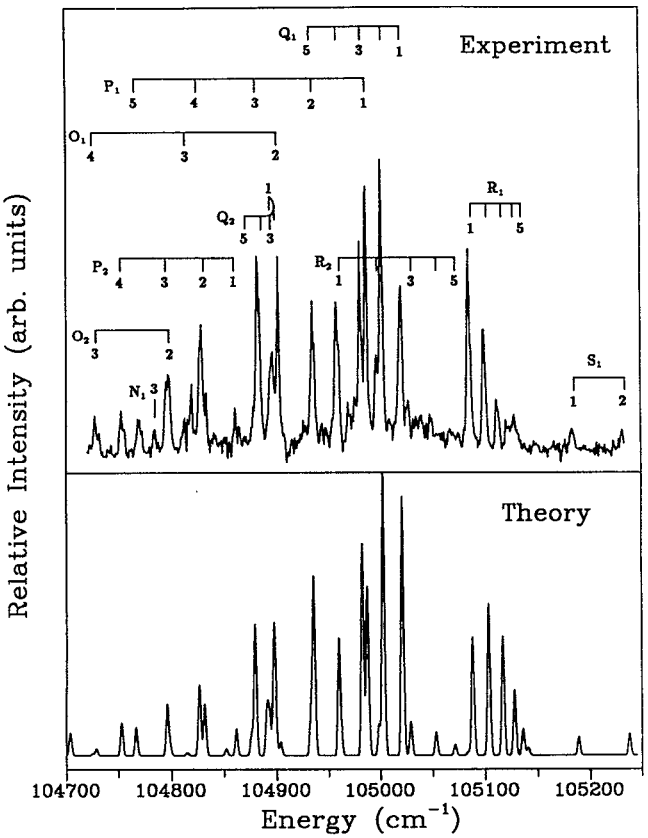

FIG. 2. The measured (top) and calculated (bottom) pulsed field ionization spectra of OH^+ ($X\,^3\Sigma^-$, $v^+=0$) from the $X\,^2\Pi_i$ ground state of OH. The branch designations refer to ΔN and the subscript designates whether the transition originates from the F_1 or the F_2 level. We do not resolve the triplet splitting in the ion. The numbers on each ladder give the value of N''.

the *f* component of the Λ doublet are observed in the formation of OH radicals.[16,17] However, they are not expected to have any residual alignment (electronic or rotational) in the present experiment due to collisions with background gases in the flow tube. The photoelectron spectra were calculated assuming a Boltzmann distribution at 220 K and convoluted with a Gaussian detection function having a full width at half-maximum (FWHM) of 3 cm^{-1}. Previous photoionization measurements[17–19] using similar radical sources found that the product radicals were essentially thermalized with rotational temperatures of 300–400 K. However, our calculations indicate a somewhat lower temperature suggesting that there is some cooling of the products as they expand into the vacuum system through the exit aperture of the flow tube.

The peaks of Fig. 2 were assigned using energy expressions for Hund's case (b) coupling for the $X\,^3\Sigma^-$ ionic state and intermediate case (a)/(b) coupling for the $X\,^2\Pi$ ground state.[20] Rotational constants were obtained from the laser magnetic resonance work of Gruebele *et al.*[21] for OH^+ and the tabulations of Huber and Herzberg[14] for neutral OH. Assignment of the spectrum was straightforward using relative rotational transition energies calculated from the spectroscopic data noted above. The rotational branch labels in Fig. 2 have a subscript denoting the spin (*F* level) of the originating state. For the inverted neutral ground state, F_1 refers to the $^2\Pi_{3/2}$ spin–orbit state and F_2 refers to the $^2\Pi_{1/2}$ spin–orbit state which are separated by 139.2 cm^{-1} (Ref. 14). The small spin-rotation splitting in the $^3\Sigma^-$ ion is just beyond the resolution of our scans, so each ionic rotational level is labeled by N^+, which is the angular momentum apart from spin. It is convenient to associate with each branch a letter designation which refers only to the change in core angular momentum apart from spin, i.e., $\Delta N=N^+-N''$, where $N''=J''-1/2$ and $N''=J''+1/2$ for the F_1 and F_2 components of the ground state, respectively. For example, the $P_1(2)$ line represents the transition originating from the $N''=2$, $J''=5/2$, $X\,^2\Pi_{3/2}$ level and ending on the $N^+=1$, $J^+=0$, 1, and 2 levels of the ion. The transitions which end on the $J^+=1$, $N^+=0$ level have only one spin component in the upper state and can be seen to have slightly narrower peaks than the other transitions. Absolute calibration of the measured spectrum results in an ionization potential of 104 989 ± 2 cm^{-1} (13.017 eV) which corresponds to the lowest possible ionization transition, i.e., the $P_1(1)$ line. This value can be compared to lower resolution determinations by photoelectron spectroscopy (13.01 eV)[1,2] and photoionization mass spectrometry (12.99 ± 0.02 eV).[18]

The most prominent branches are the P_1, Q_1, and R_1 which one might associate with the "normal" one-photon allowed electronic transitions since $|\Delta N|\leqslant 1$. The corresponding branches originating from the F_2 components of the ground state are nearly as strong because the spin–orbit splitting is small relative to the rotational temperature. The observation of one-photon branches with $|\Delta N|>1$ (*N*, *O*, and *S*) have no counterpart in neutral–neutral electronic transitions but are a consequence of the partitioning of angular momentum between the ion core and photoelectron in the photoionization process. The S_2 branch transitions are evidently too weak to be observed and the T_1 and N_2 branches do not appear because they fall outside the scanned range. Of considerable interest in this work is the low intensity of the *S* branches compared to the *O* branches, both of which involve the same absolute change in core rotation, i.e., $|\Delta N|=2$. This feature of the data will be discussed in more detail below.

To provide further insight into the photoionization dynamics of these near-threshold spectra, Fig. 3 shows calculated rotational branching ratios [Fig. 3(b)] for photoionization of the $N''=2$, $J''=5/2$ rotational level of the $X\,^2\Pi_{3/2}$ ion along with the measured values [Fig. 3(a)]. Good agreement is seen between these spectra except for the $\Delta N=-2$ peak. The calculated $\Delta N=-2$ peak is much weaker than the measured value. The asymmetry observed in these branch intensities, where negative ΔN (ΔJ) branches are uniformly more intense than the corresponding positive ΔN (ΔJ) branches, has also been observed in the threshold photoionization spectra of N_2O (Ref. 22) and HCl (Refs. 23 and 24). This behavior is also evident in several (1+1′) REMPI threshold photoelectron measurements on NO via rotational levels of the $A\,^2\Sigma^+(3s)$ Rydberg state.[25–27] Although the calculated spectra of Figs. 2

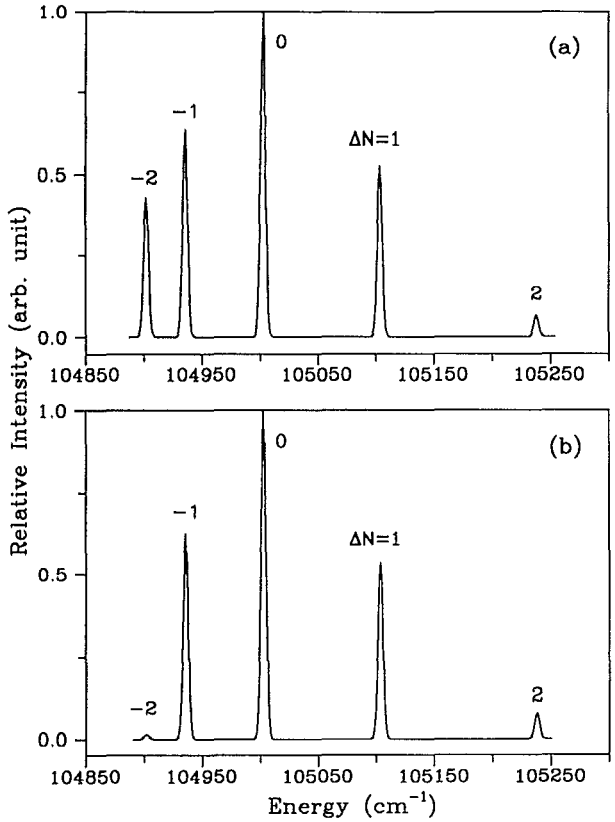

FIG. 3. The measured (a) and calculated (b) rotational branching ratios of OH^+ ($X\,^3\Sigma^-$, $v^+=0$) from the $N''=2$, $J''=5/2$ rotational level of the $X\,^2\Pi_i$ ground state of OH. Both spectra are convoluted with a Gaussian detection function with an FWHM of 5 cm^{-1}. A kinetic energy of 25 meV and no alignment in the ground rotational levels of OH are assumed in the calculations.

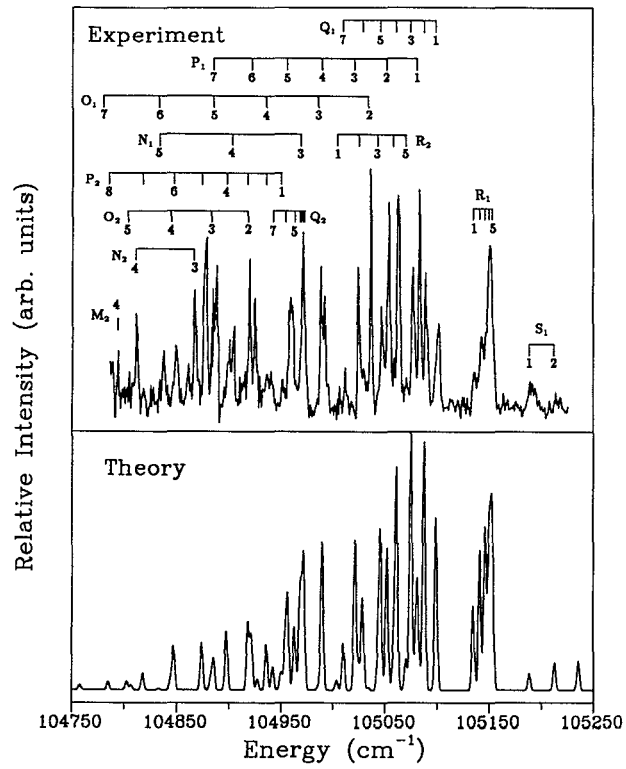

FIG. 4. The measured (top) and calculated (bottom) pulsed field ionization spectra of OD^+ ($X\,^3\Sigma^-$, $v^+=0$) from the $X\,^2\Pi_i$ ground state of OD. The branch designations refer to ΔN and the subscript designates whether the transition originates from the F_1 or the F_2 level. We do not resolve the triplet splitting in the ion. The numbers on each ladder give the value of N''.

and 3 show slightly larger intensity for the $\Delta N=-1$ peak than the $\Delta N=1$ transition, they clearly do not account for the strong asymmetry seen in the measured spectra for the $\Delta N=+2$ and -2 peaks.

To account for these unusual branch intensities, it is necessary to involve a mechanism which depends not on the final state of the ion (N^+ or J^+) but rather on the ionization path, i.e., rotational branch. One possible mechanism involves the interaction of the high-n Rydberg states ($n>150$) with lower-n Rydberg levels ($20<n<80$) converging to higher rotational state thresholds of the cation. Although these interactions are expected to be weak due to the poor overlap of the high-n Rydberg levels with more compact low-n orbitals, the level density of these states is such that energy resonances are likely to occur within the 2 cm^{-1} experimental bandwidth. Although the low-n Rydberg levels lie too far below their respective thresholds to be field ionized, these levels can autoionize once the external pulsed field is applied and the high-n Rydberg states become open ionization channels. For branches which involve relatively large negative changes in core angular momentum, i.e., O and N branches, a greater number of isoenergetic low-n states will be optically connected to the ground state than for S and T branches due to the lower changes required in angular momentum. Pulsing the extraction field ionizes the high-n Rydberg levels and simultaneously allows the isoenergetic low-n Rydberg states to autoionize into this new open continuum channel. As a result, the branches with large negative ΔJ have the greatest probability for enhanced intensity relative to branches with positive ΔJ, in qualitative agreement with the OH (OD) and other threshold photoionization measurements. Similar mechanisms involving Rydberg state interactions have been proposed to account for the enhancement of $\Delta N<0$ transitions found in the $(1+1')$ REMPI threshold spectra of NO (Ref. 27) and the observation of type a rotational transitions in the threshold photoionization spectrum of H_2O.[28] In the case of H_2O, however, a recent *ab initio* calculation[29] demonstrates that type a transitions are mainly due to the direct molecular photoionization process itself and not to rotational autoionization. This mechanism is discussed in detail in the case of the threshold spectra of HCl (Ref. 23) where spectral congestion is less severe than in the present case of OH and OD.

B. Photoelectron spectra of OD

Figure 4 shows measured and calculated photoelectron spectra for single-photon ionization of the 1π orbital of neutral OD leading to the ground ionic state. A photoelec-

tron kinetic energy of 25 meV is assumed in the calculation. The calculated spectrum is convoluted with a Gaussian detection function with an FWHM of 3 cm^{-1}. Since the photoelectron continuum is not expected to be influenced by isotopic substitution, the OD calculation uses the same photoelectron matrix elements as for photoionization of OH. The rotational constant of OD is about half that of OH (Ref. 14) and as a result the OD spectra are more congested and appear "hotter" due to the shift of population into higher N'' states. However, a rotational temperature of 220 K is still used for OD in these calculations. The observed spectrum of OD in Fig. 4 has many elements in common with the OH spectrum: the S_2 branch is not seen due to low intensity, the S_1 branch has significantly less intensity than the other branches, and many branch transitions with $\Delta N < -1$ are evident. Note that in the observed OD spectrum, the N_2 and M_2 branches appear in addition to all the branches seen in the OH spectrum. The calculated spectrum for OD is in less satisfactory agreement with the measured values than for OH. This is due in part to the larger number of lines in the OD spectra as a result of the lower rotational constants for the neutral and cation. Rotational autoionization seems more important for OD since the rotational branch intensities for larger negative ΔN are negligible in the calculated spectra. The ionization potential of OD obtained from the position of the $P_1(1)$ transition ($N^+=0$, $J^+=1 \leftarrow N''=1$, $J''=3/2$) is $105\,085 \pm 2$ cm^{-1}.

ACKNOWLEDGMENTS

Work at Brookhaven National Laboratory was supported by the U.S. Department of Energy, Office of Basic Energy Sciences under Contract No. DE-AC02-76CH00016. Work at the California Institute of Technology was supported by grants from the National Science Foundation, Air Force Office of Scientific Research, and the Office of Health and Environmental Research of the U.S. Department of Energy. We also acknowledge use of resources of the Jet Propulsion Laboratory/Caltech CRAY Y-MP2E/116 Supercomputer.

[1] S. Katsumata and D. R. Lloyd, Chem. Phys. Lett. **45**, 519 (1977).
[2] H. Van Lonkhuyzen and C. A. de Lange, Mol. Phys. **51**, 551 (1984).
[3] E. de Beer, M. P. Koopmans, C. A. de Lange, Y. Wang, and W. A. Chupka, J. Chem. Phys. **94**, 7634 (1991).
[4] E. de Beer, C. A. de Lange, J. A. Stephens, K. Wang, and V. McKoy, J. Chem. Phys. **95**, 714 (1991).
[5] G. Reiser, W. Habenicht, K. Müller-Dethlefs, and E. W. Schlag, Chem. Phys. Lett. **152**, 119 (1988).
[6] R. G. Tonkyn, J. W. Winniczek, and M. G. White, Chem. Phys. Lett. **164**, 137 (1989).
[7] K. Wang and V. McKoy, J. Chem. Phys. **95**, 4977 (1991).
[8] J. A. Silver, W. L. Dimpfi, J. H. Brophy, and J. L. Kinsey, J. Chem. Phys. **65**, 1811 (1976).
[9] K. R. German and R. N. Zare, Phys. Rev. **186**, 9 (1969).
[10] R. H. Page, R. J. Larkin, A. H. Kung, Y. R. Shen, and Y. T. Lee, Rev. Sci. Instrum. **58**, 1616 (1987).
[11] T. P. Softley, W. E. Ernst, L. M. Tashiro, and R. N. Zare, Chem. Phys. **116**, 299 (1987).
[12] R. G. Tonkyn and M. G. White, Rev. Sci. Instrum. **60**, 1245 (1989).
[13] I. Dabrowski and G. Herzberg, Can. J. Phys. **52**, 1110 (1974).
[14] K. P. Huber and G. Herzberg, *Molecular Spectra and Molecular Structure IV. Constants of Diatomic Molecules* (Van Nostrand, New York, 1979).
[15] J. A. Stephens and V. McKoy, J. Chem. Phys. **88**, 1737 (1988).
[16] R. Vasudev, R. N. Zare, and R. N. Dixon, J. Chem. Phys. **80**, 4863 (1984).
[17] A. M. L. Irvine, I. W. M. Smith, R. P. Tuckett, and X.-F. Yang, J. Chem. Phys. **93**, 3177 (1990).
[18] P. M. Dehmer, Chem. Phys. Lett. **110**, 79 (1984).
[19] P. M. Dehmer, J. Berkowitz, and W. A. Chupka, J. Chem. Phys. **59**, 5777 (1973).
[20] G. Herzberg, *Molecular Spectra and Molecular Structure I. Spectra of Diatomic Molecules* (Van Nostrand, New York, 1950).
[21] M. H. W. Gruebele, R. P. Müller, and R. J. Saykally, J. Chem. Phys. **84**, 2489 (1986).
[22] R. T. Wiedmann, R. G. Tonkyn, E. R. Grant, and M. G. White, J. Chem. Phys. **95**, 746 (1991).
[23] R. G. Tonkyn, R. T. Wiedmann, and M. G. White, J. Chem. Phys. **96**, 3696 (1992).
[24] K. S. Haber, Y. Jiang, G. P. Bryant, E. R. Grant, and H. Lefebvre-Brion, Phys. Rev. A **44**, 5331 (1991).
[25] M. Sander, L. A. Chewter, K. Müller-Dethlefs, and E. W. Schlag, Phys. Rev. A **36**, 4543 (1987).
[26] M. Takahashi, H. Ozeki, and K. Kimura, Chem. Phys. Lett. **181**, 255 (1991).
[27] G. Reiser and K. Müller-Dethlefs, J. Phys. Chem. **96**, 9 (1992).
[28] R. D. Gilbert and M. S. Child, Chem. Phys. Lett. **287**, 153 (1991).
[29] M.-T. Lee, K. Wang, V. McKoy, R. G. Tonkyn, R. T. Wiedmann, E. R. Grant, and M. G. White, J. Chem. Phys. (in press).